Electronic structure calculations of hexagonal and cubic phases of Co_3Pt

S. D. Willoughby,[a] R. A. Stern, R. Duplessis, and J. M. MacLaren
Department of Physics, Tulane University, New Orleans, Louisiana 70118

M. E. McHenry and D. E. Laughlin
Department of Materials Science and Engineering, Carnegie Mellon University, Pittsburgh, Pennsylvania 15213

(Presented on 13 November 2002)

Using first principles electronic structure calculations we investigated structural and magnetic properties of three distinct phases of Co_3Pt. Relaxed lattice constants, total energies, magnetocrystalline anisotropies, and density of states were calculated for each phase at their equilibrium lattice constants, as well as under expansion and contraction stresses. These computations may help clarify the results of some recent but ambiguous experiments on Co_3Pt.
© *2003 American Institute of Physics.* [DOI: 10.1063/1.1556200]

I. INTRODUCTION

Co–Pt alloys have been the focus of much recent research, partly because one phase of this material possesses high magnetocrystalline anisotropy (MCA). Co_3Pt is particularly appealing as a material for high density data storage because of increased cost effectiveness due to less Pt than traditional Co–Pt alloys, while retaining a high MCA and large magnetization.

Groups have reported MCAs of 15×10^6 ergs/cm^3,[1] up to 26×10^6 ergs/cm^3,[2] yet there has been some difficulty physically characterizing these films. It has been suggested that a mixture of hexagonal and cubic phases is often formed during growth.[1] Harp *et al.* suggested that partially ordered, alternating layers of Co followed by a mixed layer of half cobalt and half Pt form the overall structure,[3] and this type of layering would naturally give rise to the magnetic effects seen.

Researchers have grown these films on a variety of substrates. Films grown on $Al_2O_3(0001)$ have yielded some of the higher MCAs, with one reported value of 21×10^6 ergs/cm^3.[4] Groups have also used substrates of $Al_2O_3(11\bar{2}0)$, MgO(111), fused silica, sapphire(0001), and Ru(0001) with success. Another important factor in yielding a film with high MCA is the growth temperature, with temperatures in the range of 300–400 °C yielding the high MCA phases.[1,2] Higher temperatures allow atomic diffusion and the formation of the thermodynamically stable cubic phase. Films grown above a certain cutoff temperature show no MCA at all, presumably due to growth of a film that is purely cubic in structure. This cutoff appears to be between 430 and 500 °C.[3,5] Bandhu *et al.* have examined the elastic properties of several epitaxial Co_3Pt films grown at different temperatures on a sapphire (0001) substrate and concluded that the different magnetic properties reported can not be attributed to macroscopic anisotropic strain.[6]

We have performed *ab initio* calculations on three phases of Co_3Pt, shown in Fig. 1. As can be seen in the figure, the DO_{19} hexagonal phase consists entirely of mixed layers of 75% Co and 25% Pt. The fcc derivative $L1_2$ [along the (111) axis] consists of all mixed layers as well. In contrast, the orthorhombic $Pmm2$ phase possesses a pure Co layer followed by a mixed layer containing half Co and half Pt. For each ordered phase, we have calculated relaxed atomic structures, total energies, density of states, and magnetocrystalline anisotropies. These properties were also cal-

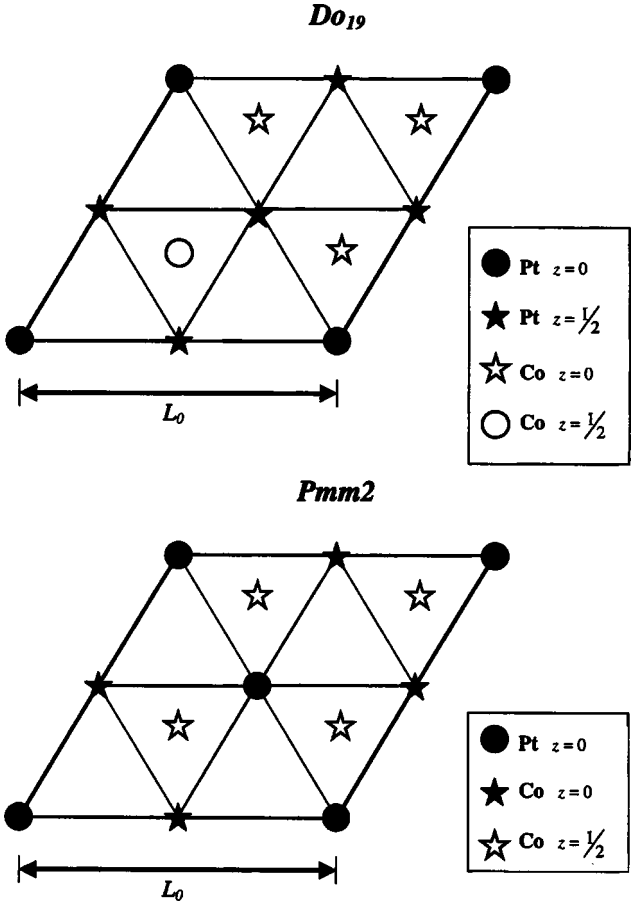

FIG. 1. Basic stacking for DO_{19} (top) and $Pmm2$ phases.

[a]Electronic mail: swillou@tulane.edu

 © 2003 American Institute of Physics

TABLE I. Energy differences per atom for DO_{19}, $L1_2$, and $Pmm2$.

Phase (L_0 Å)	Total energy/atom (eV)	Energy diff. (vs. $L1_2$)
$DO_{19}-1\%$	−6.769	0.034
$L1_2-1\%$	−6.803	
$Pmm2-1\%$	−6.775	0.028
DO_{19} g.s. (5.208)	−6.771	0.027
$L1_2$ g.s. ($5.227/\sqrt{2}$)	−6.798	
$Pmm2$ g.s. (5.227)	−6.779	0.019
$DO_{19}+1\%$	−6.766	0.014
$L1_2+1\%$	−6.780	
$Pmm2+1\%$	−6.776	0.003

culated for each structure with a 1% compression and a 1% expansion to simulate growth on different substrates. MCA's were calculated for a fully disordered hexagonal phase using the lattice constants from the $Pmm2$ phase. Total energies were used to study energy differences between all structures considered.

II. THEORY

In order to examine the energy differences between the phases studied, we made use of two *ab initio* methods. Structural relaxations and total energies were obtained with the Vienna *ab initio* Simulation Package (VASP),[7] using the projector augmented wave all-electron potentials[8] and the generalized gradient approximation to the exchange-correlation potential.[9] Equilibrium lattice constants were obtained by minimizing the total energy with respect to structure. Strained lattice constants were found by expanding/compressing the lattice constant by 1%, and then minimizing the energy with respect to c/a.

Total energies were calculated both with VASP and with the layer Korringa–Kohn–Rostoker method (LKKR).[10,11] The LKKR method uses the atomic spheres approximation, and the local density approximation to the exchange-correlation potential. Implemented in the LKKR code is the coherent potential approximation,[12] which was used to treat the fully disordered hexagonal phase. Using the CPA within LKKR allows us to calculate disordered alloys within the same set of approximations as the ordered alloys. In common with previous work,[13] the MCA was calculated with LKKR using the force theorem.[14] In order to calculate the MCA, the potentials are converged without spin-orbit coupling. After convergence is reached, spin-orbit coupling is turned on, and the frozen potentials are used to calculate the band sum energy with the magnetization pointed along the easy then hard axes of magnetization, the difference of these two energies yielding the magnetocrystalline anisotropy. For all calculations, total energies were converged with respect to *k*-points and energy points to better than 1 meV/atom.

III. RESULTS

Table I shows the total energy per atom for the different phases in their ground state configuration, expanded and contracted lattice, as well as the energy difference relative to the cubic phases. Also shown in Table I are the calculated relaxed lattice constants for each phase. The energy of the DO_{19} phase is higher than either of the other phases for all cases considered. The disordered total energy, (not shown) calculated with the LKKR method was found to have a higher total energy than the $Pmm2$ or $L1_2$ phases. As shown in the table, the cubic phase yields the lowest total energy per atom for all configurations considered so far. However, when the cubic and $Pmm2$ phases are both expanded by 1%, the energy difference between the two phases is reduced considerably, while a 1% compression yields a larger energy difference between the phases. This suggests that growth on a substrate that causes expansion of the basal plane lattice constant is a possible route to preferential growth of the orthorhombic $Pmm2$ phase of Co_3Pt.

TABLE II. Calculated values of magnetocrystalline anisotropy ($\times 10^6$ erg/cm^3).

Phase	LKKR	Néel model
$Pmm2$	28.27	17.14
DO_{19}	−28.48	−20.94
disordered	−39.12	−1.42
Co–Co interaction	Co–Pt interaction	General expression
L_1	L_2	$Pmm2$: $0.445*L_1-1.055*L_2$
−30	−31	DO_{19}: $-0.897L_1+1.63*L_2$

Magnetocrystalline anisotropies were calculated with the LKKR method, as well as within the Néel model.[15] The Néel model is restricted to nearest neighbors, and has been used successfully in the past to examine anisotropies of superlattices.[13] Within the Néel model, the anisotropy energy is proportional to $\cos^2(\theta)$ where θ is the angle between the easy axis and the chosen magnetization direction. Values calculated for the phases within the Néel model and in LKKR are presented in Table II. MCAs calculated with the LKKR method used the experimental lattice constant.[4] The parameters L_1 and L_2 also shown in Table II along with the general expression used for the calculations were taken from previous CoPt and CoPd superlattice calculations.[13] In the general expression for the Néel model MCA $[E\sim L/2\Sigma(\mathbf{m}\cdot\mathbf{r})^2/r^2]$, $\mathbf{m}$ is the chosen direction of magnetization, $\mathbf{r}$ is the vector pointing from one atom to its neighbor, and L corresponds to the type of interaction being considered. The $L1_2$ phase possesses no anisotropy as it is cubic. The LKKR calculations are consistent with the Néel model findings of $Pmm2$ having an out of plane anisotropy, and the DO_{19} having an in-plane anisotropy. One anisotropy obtained from LKKR calculations for the $Pmm2$ phase is within the range of anisotropies that have been seen experimentally. It was difficult for the Néel model to treat the disordered phase, possibly due to a nearly ideal c/a. Presumably, the high MCA in the $Pmm2$ is caused by the interface formed between the pure Co layer and the mixed layer.

Density of states were calculated with both VASP and LKKR, with the VASP results shown in Fig. 2. Both methods yielded very similar density of states for each of the phases. All three phases of Co_3Pt are strong ferromagnets and appear to have a filled majority band. Thus changes affected by distortion will change the character of the minority band.

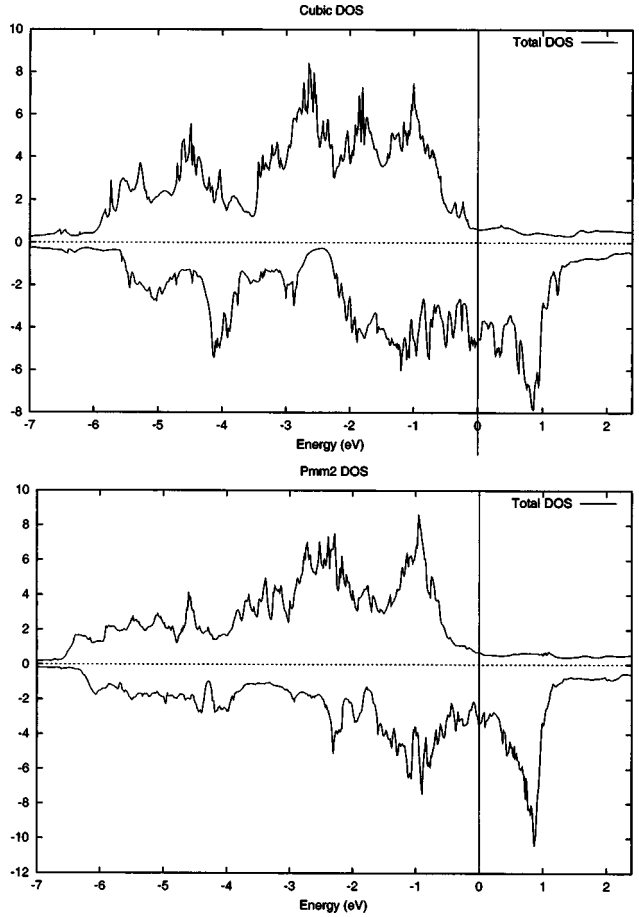

FIG. 2. Total density of states for the $L1_2$ and $Pmm2$ phases of Co_3Pt.

Density of states calculated for the expanded lattices exhibit a small increase in the weight of the minority band below the Fermi energy for the $Pmm2$ phase, which is consistent with some stabilization of this phase. The density of states for the cubic phase at an expanded lattice constant looks quite similar to the ground state, while for a contracted lattice it shows small changes in the minority band below the Fermi energy, suggesting a mechanism for stabilization of this phase upon contraction. It is possible that the use of a substrate with a slightly larger lattice constant in the basal plane will result in preferential growth of the $Pmm2$ phase. This was also suggested by the smaller energy differences seen between the $L1_2$ and the $Pmm2$ upon a 1% expansion of the relaxed lattice.

IV. CONCLUSIONS

Three phases of Co_3Pt have been studied via *ab initio* electronic structure calculations. Relaxed lattice constants were calculated for all ordered phases. The fcc derivative $L1_2$ phase was found to have the lowest total energy per atom compared to the other phases for all configurations examined so far. However, the energy difference per atom between the $L1_2$ phase and the orthorhombic $Pmm2$ phase is seen to decrease when each phase undergoes a 1% expansion from their respective ground state configurations. Calculated magnetocrystalline anisotropies roughly agree with the Néel model, and the $Pmm2$ anisotropy is within the range of anisotropies seen experimentally for Co_3Pt films. The $L1_2$ phase exhibits no anisotropy, and the DO_{19} was found to have an in-plane anisotropy. Density of states calculations reveal that all three phases have a full majority band, so electronic changes made to the configurations of the phases affect the minority bands, and the density of states for a 1% lattice expansion reveal changes suggesting stabilization of the $Pmm2$ phase.

ACKNOWLEDGMENTS

This research was supported by the National Science Foundation, Grant Nos. DMR-9971573 and 2001-04-RII-03.

[1] Y. Yamada, T. Suzuki, and E. Abarra, IEEE Trans. Magn. **34**, 343 (1998).
[2] M. Maret, M. Cadeville, A. Herr, and P. Poinsot, J. Magn. Magn. Mater. **191**, 61 (1999).
[3] G. Harp, D. Weller, T. Rabedeau, R. Farrow, and M. Toney, Phys. Rev. Lett. **71**, 2493 (1993).
[4] Y. Yamada and T. Suzuki, Mater. Res. Soc. Symp. Proc. **517**, 299 (1998).
[5] Y. Yamada, W. V. Drent, E. N. Abarra, and T. Suzuki, J. Appl. Phys. **83**, 6527 (1998).
[6] R. Bandhu, R. Sooryakumar, R. Farrow, D. Weller, and M. Toney, J. Appl. Phys. **91**, 2737 (2002).
[7] G. Kresse and J. Furthmuller, Vienna ab initio Simulation Package (2001), http://cms.mpi.univie.ac.at/vasp/
[8] G. Kresse and J. Joubert, Phys. Rev. B **59**, 1758 (1999).
[9] J. Perdew, K. Burke, and M. Ernzerhof, Phys. Rev. Lett. **77**, 3865 (1996).
[10] J. MacLaren, S. Crampin, and D. Vvendensky, Phys. Rev. B **40**, 12176 (1989).
[11] J. MacLaren, D. Vvendensky, R. Albers, and J. Pendry, Comput. Phys. Commun. **60**, 365 (1990).
[12] J. MacLaren, A. Gonis, and G. Schadler, Phys. Rev. B **45**, 14392 (1992).
[13] R. Victora and J. MacLaren, Phys. Rev. B **45**, R11583 (1993).
[14] A. Makintosh and O. Anderson, *Electrons at the Fermi Surface* (Cambridge University Press, London, 1980).
[15] L. Néel, J. Phys. Radium **15**, 225 (1954).